SAND78-1088
Unlimited Release

Midtemperature Solar Systems Test Facility (MSSTF) Project Test Results: Phase IVA MSSTF System Operation

Thomas D. Harrison, William H. McCulloch

Prepared by Sandia Laboratories, Albuquerque, New Mexico 87185
and Livermore, California 94550 for the United States Department
of Energy under Contract AT(29-1)-789

Printed November 1978

Sandia Laboratories

SF 2900 QD (4-78)

Issued by Sandia Laboratories, operated for the United States Department of Energy by Sandia Corporation.

NOTICE

Printed in the United States of America

Available from
National Technical Information Service
U. S. Department of Commerce
5285 Port Royal Road
Springfield, VA 22161

Price: Printed Copy $5.25 ; Microfiche $3.00

SAND78-1088
Unlimited Release
Printed November 1978

MIDTEMPERATURE SOLAR SYSTEMS TEST FACILITY (MSSTF) PROJECT TEST RESULTS: PHASE IVA MSSTF SYSTEM OPERATION

Thomas D. Harrison
William H. McCulloch
Midtemperature Solar Systems Test Division 4721
Sandia Laboratories
Albuquerque, NM 87185

ABSTRACT

This report summarizes the results of 21 months of testing a dispersed power system that converts solar energy to electrical and thermal energy during Phase IVA at the Midtemperature Solar Systems Test Facility (MSSTF), Albuquerque, New Mexico. It presents data showing that the production of both electrical and thermal energy from solar energy is technologically feasible. Operational experience with the MSSTF has led to the identification of several design modifications and materials and process improvements that will increase system efficiency. System performance is reported both as measured for the existing system and as predicted for a system incorporating the identified improvements.

CONTENTS

ILLUSTRATIONS

2

ILLUSTRATIONS (cont)

TABLES

MIDTEMPERATURE SOLAR SYSTEMS TEST FACILITY (MSSTF) PROJECT TEST RESULTS: PHASE IVA MSSTF SYSTEM OPERATION

Introduction

This report summarizes the results of testing the Department of Energy's (DOE's) Midtemperature Solar Systems Test Facility (MSSTF) at Sandia Laboratories, Albuquerque, New Mexico.[1] The system is a dispersed power system that collects solar energy and supplies both the electrical and thermal energy demands of a representative load. Testing was done between July 1976 and March 1978.

History of the MSSTF Project

As shown in Figure 1, the MSSTF Project began in FY73. A collector field subsystem, thermal storage subsystem, fluid-transfer facility, prime-mover subsystem, heating-and-cooling subsystem, and control and data-acquisition equipment have been installed. As of March 1978, data are being collected on the MSSTF as an operating system. The system as presently configured is termed the "Phase IVA MSSTF" in this report and is shown schematically in Figure 2. Figure 2 shows the transport fluid temperatures in degrees centigrade at critical points in the system. Some of these temperatures vary according to whether the system is being operated in the summer, winter, or in maximum electrical output modes (denoted S, W, or E, respectively). Figures 3 and 4 are a schematic and an artist's concept of the system as it is expected to appear in mid-1979 for Phase IVB.

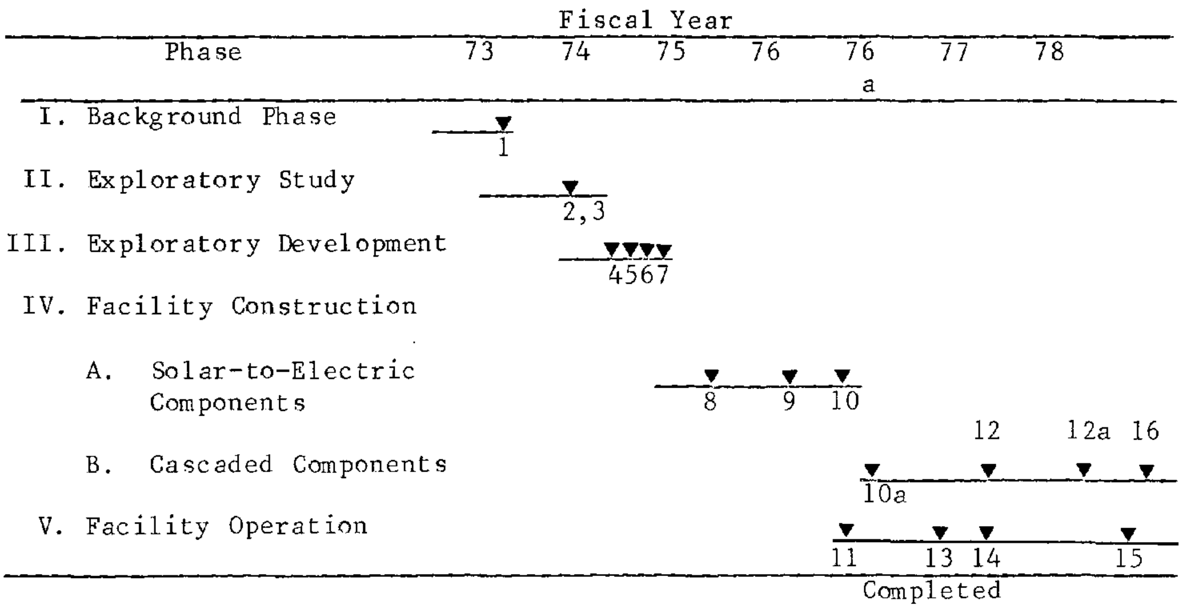

Milestones

1. Completion of Phase I
2. Preliminary System Design Complete
3. Economic Evaluation Complete, etc.
4. Collector Evaluation Facility Complete
5. System Analysis Program (SOLSYS) Operational
6. Baseline System Design Complete
7. Phase IVA Proposal Submitted
8. Phase IVA Design Freeze
9. Partial Collector Field, Storage, and Turbine-Generator Test Bed Complete--First Solar Energy Collection
10. Phase IVA Complete, System 100-percent Operational

10a. Subcontracts for Collector Field Subsystems Placed

11. Initial Operation of Partial Midtemperature Solar Systems Test Facility

Figure 1. Midtemperature Solar Systems Test Facility Project Milestones

3

12. Low-Temperature Components of Midtemperature Solar Systems Test Facility Installed

12a. Subcontracted Collector Field Subsystems Completed

13. System Analysis Program (SOLSYS) Refined and Revalidated

14. Demonstration of Solar Project Building

15. Operation of Complete Midtemperature Solar Systems Test Facility

16. New Collector Field Design Initiated

Figure 1 (cont)

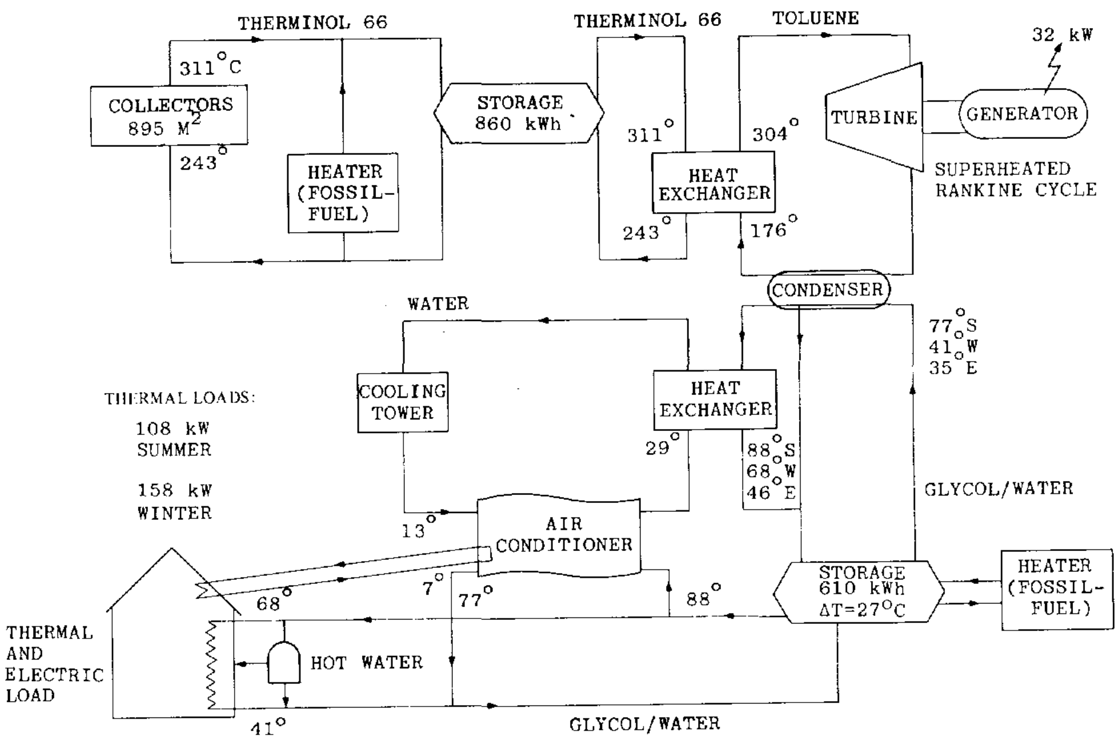

Figure 2. Simplified Schematic, Phase IVA MSSTF

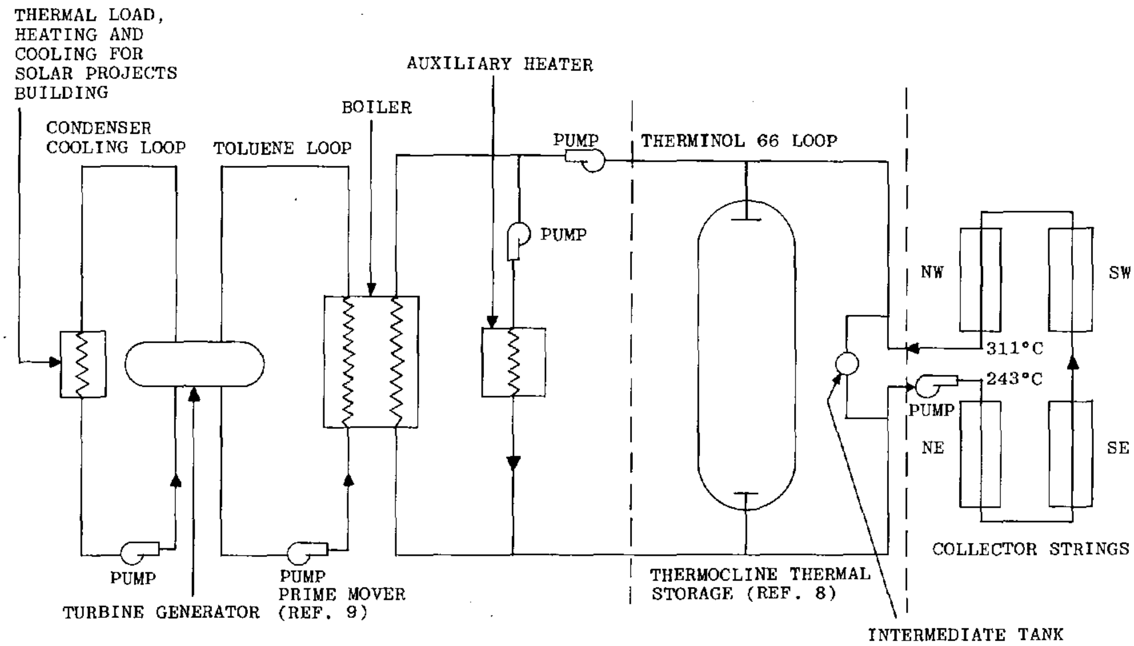

Figure 3. Phase IVB Midtemperature Solar Systems Schematic

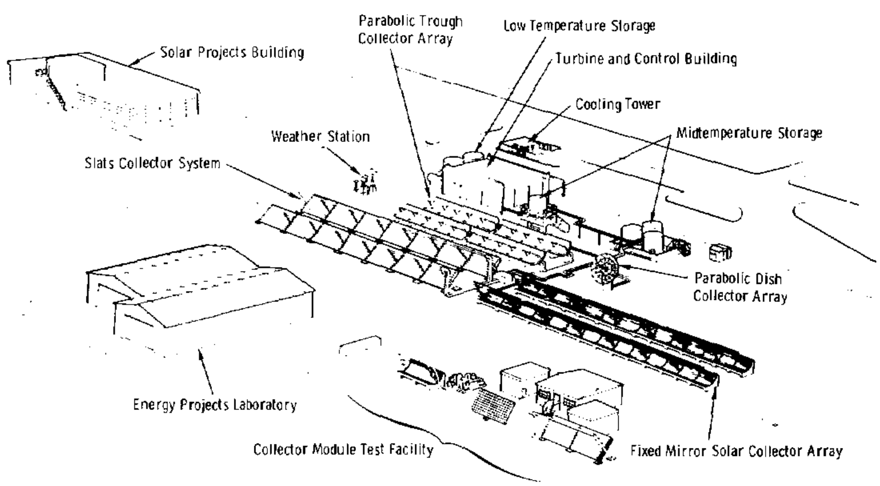

Figure 4. Phase IVB Midtemperature Solar Systems Test Facility

Purpose of the Report

The purpose of this report is to acquaint the reader with the MSSTF project, to describe the elements of the system that comprise the Phase IVA MSSTF, and to report the data and experiences obtained from operation of the Phase IVA MSSTF. Testing included evaluating the various subsystems and components of the MSSTF and how well they operate together when incorporated into a system to produce usable energy from solar power. System evaluation will be presented in the following sequence.

1. Establish an inventory for the thermal energy collected.

2. Review test data on the subsystems and components that comprise the system.

3. Identify problems and their solutions.

4. Project performance for the Phase IVB MSSTF.

Objectives of the MSSTF

The DOE established the MSSTF to perform the testing and engineering evaluation required as part of the national plan to achieve commercial application of solar thermal technology in the 200° to 400°C range for dispersed solar thermal power applications by the mid-1980s. The relationship of test and evaluation activities to the other steps toward commercialization is shown in Figure 5.

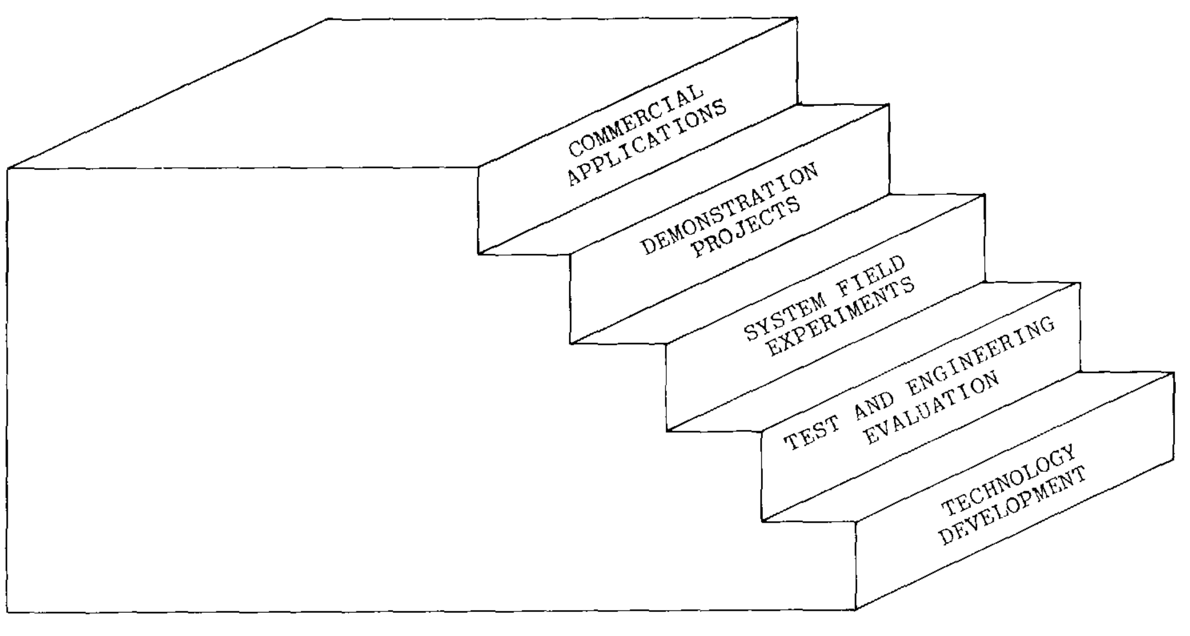

Figure 5. Steps Toward Commercialization of Solar Power Systems

The goals for the MSSTF may be summarized as follows:

1. Characterize with representative engineering tests candidate solar energy components and subsystems.

2. Integrate experimental hardware into representative solar energy systems; i.e., systems large enough to encounter the problems of integrating full-scale components, to establish the feasibility of the solar total energy concept, and to provide technical and cost data for solar total energy and other dispersed power systems.

3. Analyze the experimental data (from the MSSTF and other sources) to formulate helpful conclusions in designing systems for large-scale experiments, demonstrations, and commercial applications.

4. Disseminate the results and conclusions through reports, seminars, conferences, tours, briefings, and technical interchanges with visitors at the MSSTF.

Test Reports Published by the MSSTF Project

This test summary on systems operations is part of the effort that satisfies the last goal, Disseminate. Summary test reports are published annually on the Collector Module Test Facility (CMTF) and the System Test Facility (STF) (which comprise the MSSTF) as well as on four subsystems of the STF:

1. The Collector Field
2. High-Temperature Thermal Storage, including fluid-transfer equipment
3. The Prime Mover
4. Heating and Cooling Equipment

In addition, a semiannual status report on the overall MSSTF project is published.

4

Test Results

The following paragraphs describe the results of 21 months of testing on the Phase IVA MSSTF.

Description of the Phase IVA MSSTF

The Phase IVA MSSTF covered in this report consists of

- A 200-m^2 (2160-ft^2) east-west parabolic trough collector field subsystem, which collects a measured 431-kWh thermal on a typical winter day and an estimated 483 kWh on a typical summer day.

- A high-temperature thermocline storage subsystem, capable of storing 278-kWh thermal energy in Therminol 66 between 240°C and 310°C.

- Fluid-transfer equipment, including piping, pumps, and valves.

- A prime-mover subsystem to convert thermal energy to electrical energy.

- A control and data-acquisition system.

A brief description of each of these elements follows.

200-m^2 East-West Parabolic Trough Collector Field Subsystem -- This subsystem, designed by Sandia, consists of four 18.3-m (60-ft)-long by 2.7-m-(9-ft)-wide parabolic troughs in two rows along an east-west (E-W) axis (Figure 6). Reflective surfaces of the collectors are aluminized Teflon laminated to Mylar and bonded to aluminum sheet. The reflectors are attached to plywood troughs with spring-loaded edge clamps and screws. The steel receiver tubes are coated with highly absorptive black chrome, are sealed in glass tubing, and extend the full length of each set of troughs. Tracking and control of the collector field is done with a minicomputer that compares collector elevation angle with a sun position program and sends appropriate correction signals to the drive motors.

High-Temperature Thermocline Storage Subsystem -- This storage subsystem (Figure 7) stores both high-temperature (310°C) and low-temperature (240°C) Therminol 66 (T-66) a product of Monsanto Chemical Company, in the same tank. The low- and high-temperature fluids are separated by the difference in their densities. The capacity of the tank, 5.0 m^3 (1350 gal), enables the storage of 278 kWh thermal between 310°C and 240°C. The tank is insulated with an evacuated multifoil blanket. Diffusers minimize turbulence at the entrance and exit to avoid mixing of the low- and high-temperature fluids.

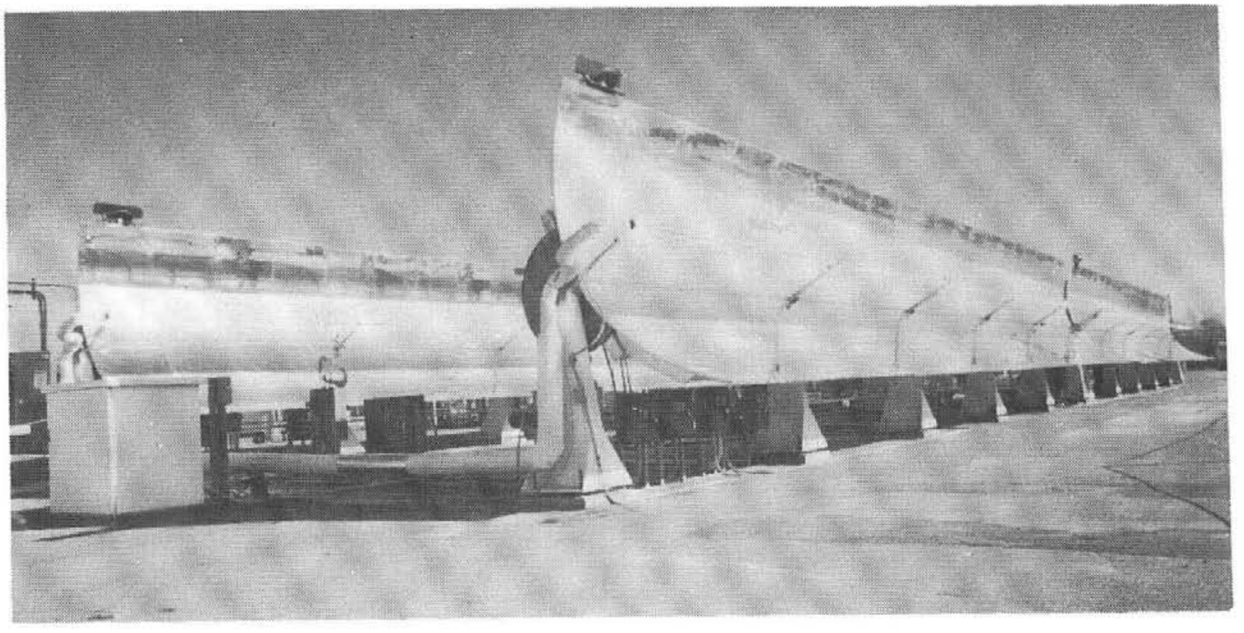

Figure 6. 200-m^2 East-West (E-W) Parabolic Trough Collector Field Subsystem

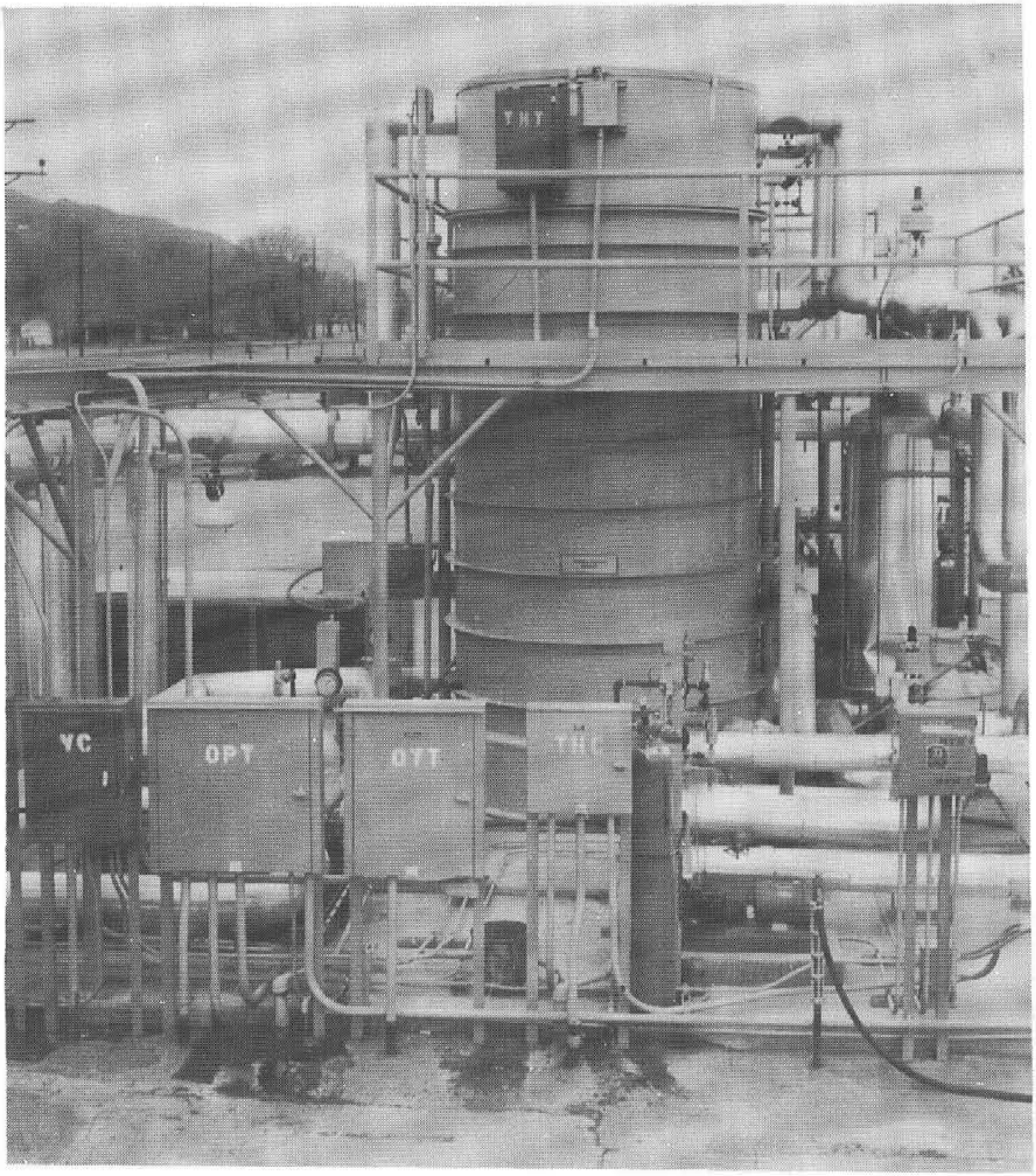

Figure 7. High-Temperature Thermocline Thermal Storage Subsystem

Fluid-Transfer Equipment -- The fluid-transfer equipment interconnects all facility subsystems and consists of valves, pumps, insulated pipelines, and flow sensors. The T-66 heat-transfer fluid for the collector field and high-temperature storage tanks is a high-boiling-point oil that remains liquid at system working temperatures - about 315°C (600°F).

Prime-Mover Subsystem -- The prime-mover subsystem (Figure 8) consists of two major elements: the toluene heat exchanger and the turbine/generator.

1. Toluene Heat Exchanger -- The heat exchanger is the interface between the heat-transfer fluid (T-66) and the turbine working fluid (toluene). Heat transfer to the toluene is accomplished in four steps -- one for preheating, two for boiling, and one for superheating. The toluene is heated to 295°C (563°F) and 1.9 MPa (275 psi) and enters the turbine as super-heated high-pressure gas.

2. Turbine/Generator -- The single-stage Organic Rankine Cycle (ORC) turbine is driven at 25,000 rpm by the toluene gas. Reduction gears drive the generator at 1800 rpm to produce up to 32 kW of electrical energy. The turbine-condenser coolant is a mixture of ethylene glycol and water, which is stored in low-temperature storage tanks and becomes the energy source for heating and air-conditioning components of the system. The turbine-condenser coolant temperature is set to 88°C (190°F) for air-conditioning needs, 74°C (165°F) for heating needs, and as low as possible at other times for maximum efficiency.

A dry cooling tower rejects the heat from the turbine condenser at times when that energy is not used to charge low-temperature storage or to meet the heating/cooling demands of the Solar Projects Building.

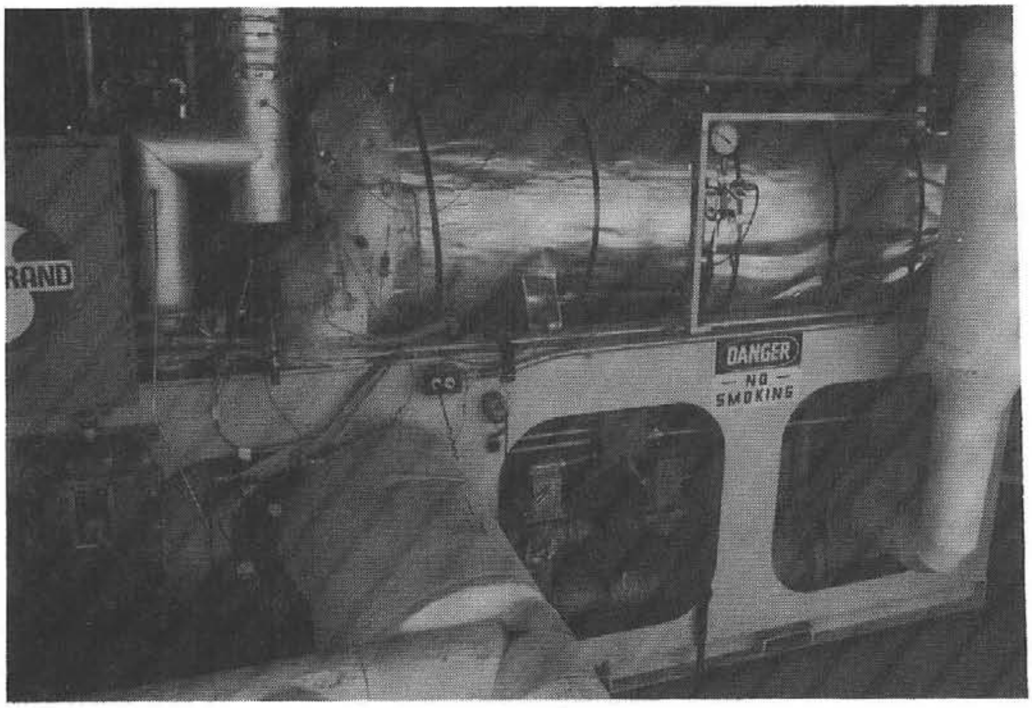

Figure 8. Prime-Mover Subsystem

Controls and Data-Acquisition Equipment -- The control and data-acquisition system (Figure 9) performs six major functions:

1. Focuses the collector (tracking and drive).
2. Controls the temperature of fluid from the collector.
3. Controls the quantity of energy to the toluene boiler.
4. Controls the quantity of energy from boiler to turbine.
5. Controls the switch to and from auxiliary heater.
6. Acquires data.

Collector focusing is done by a minicomputer that calculates the position of the sun and commands a d-c permanent-magnet motor to drive the collector trough to the correct angle. Shaft encoders provide a feedback to the computer for checking the resulting orientation. Following initial checkout, this method has been virtually troublefree.

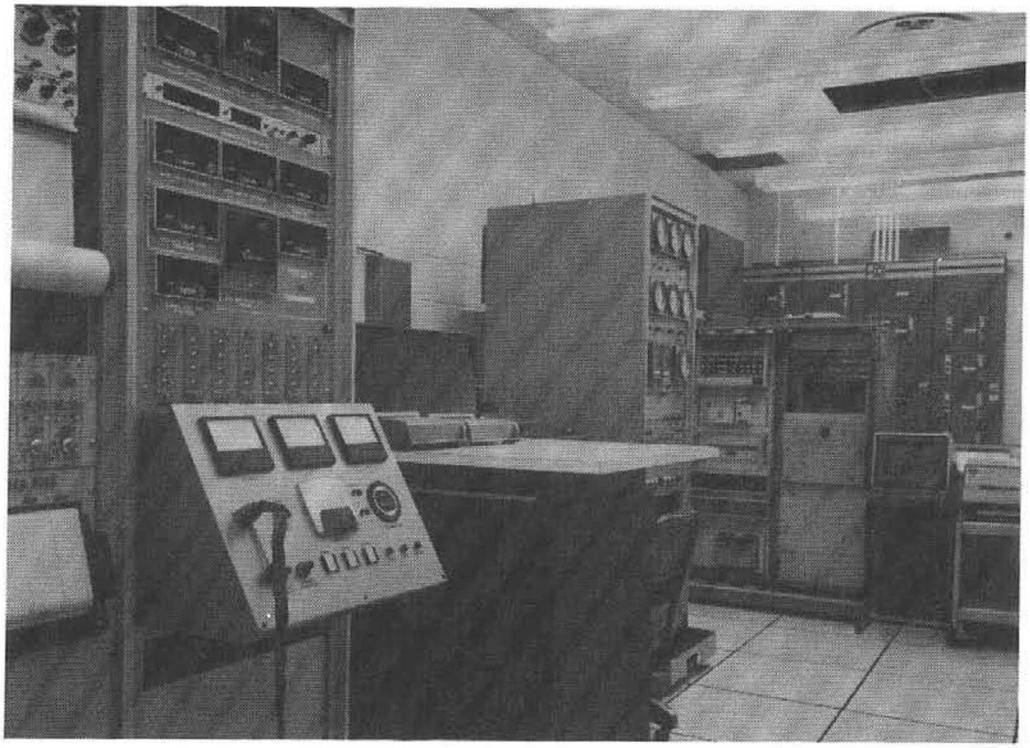

Figure 9. Control and Data-Acquisition Equipment

The temperature of the fluid leaving the collectors is controlled by the rate of flow through the receivers. A type "T" thermocouple is immersed in the fluid at the exit end. If the bulk fluid temperature is less than the specified exit temperature of 311° ±3°C, the thermocouple through electronic circuitry generates signals that slow the flow by causing the positive displacement pump to slow down. If the temperature exceeds 311° ±3°C, the thermocouple generates signals that cause the pump to speed up.

The rate of energy to the boiler is controlled by measuring the T-66 temperature at the exit side of the boiler. If the temperature is outside the limits 243° ±3°C, a positive displacement pump speeds up or slows down as required. The flow rate of fluid in and out of the thermocline storage is also controlled by this pump. If flow from the collectors cannot supply boiler needs, additional hot fluid is taken from the top of the storage tank; if flow from the collectors exceeds boiler needs, the excess is diverted by the back pressure from the boiler pump into the top of the tank.

The quantity of energy transferred from the boiler to the turbine is proportional to the flow rate of the working fluid (toluene). This flow rate is controlled by a sensor that measures the pressure upstream from the throttle. Pressure at the turbine inlet is a function of throttle setting. If an increase in load causes the turbine to slow down, the throttle opens further with a resultant drop in pressure upstream from the throttle. This drop in pressure regulates a valve in the toluene pipeline, allowing flow to increase. The toluene is moved by a centrifugal pump, which is driven by a mechanical linkage to the turbine.

A back-up fossil-fuel (gas-fired) heater supplies the energy to operate the prime mover when energy is available from neither the collectors nor the storage subsystem. When temperature sensors in the thermocline storage subsystem indicate depletion of storage, an automatic switchover is activated to turn on the heater and set up a closed T-66 loop through the heater and the toluene boiler. When storage is refilled from the collectors, the system automatically switches back to supplying heat to the toluene from storage.

In each subsystem a variety of sensors such as thermocouples, pressure gages, and flow meters are installed as needed to acquire data with which to evaluate subsystem performance. Inputs are fed to a patch panel in the control room. Up to 200 inputs (including weather data) can be fed from the patch panel into the minicomputer, which stores the data on tape, performs calculations, and provides visual readouts.

Most of the above equipment was designed and installed by Sandia Laboratories. Existing materials and technologies were used to the greatest extent possible to meet the objective of commercialization of solar power by the mid-1980s at minimum cost. All of the above equipment is large enough to provide realistic simulation of commercial systems.

Thermal Inventory of Phase IVA MSSTF

Initial design studies showed that a potentially economic use of solar energy is to use dispersed power systems to collect energy in the midtemperature (200°C to 400°C) range and cascade the energy through a "total-energy" system. The Phase IVA MSSTF passes the collected solar energy through an ORC turbine/generator to produce electricity. By operating the condenser at a higher temperature than usual, the energy ordinarily rejected as waste heat can be used for other purposes, such as heating and cooling.

With only one collector field subsystem in operation, the Phase IVA MSSTF does not collect enough energy to operate the prime mover for a full day at rated power. The procedure is to operate the prime mover from a fossil-fuel heater while the collector fills thermal storage. When storage is full, hot oil is drawn from storage to provide energy to operate the turbine. With this procedure, an all-day test of the complete system is impossible.

However, all-day tests have been conducted on each of the subsystems that comprise the Phase IVA MSSTF in accordance with the test plan.[2] An energy inventory was developed for a day typical of the winter season using the results of tests conducted on subsystems during the winter. There is no assurance with this procedure that the tests were all done under the same conditions.

For a typical clear winter day in Albuquerque, the integrated direct normal solar radiation is 7.75 kWh/m^2 or 1550 kWh over the 200 m^2 aperture of the East-West parabolic collector trough. The collector is designed to convert 38.4% of solar energy to thermal energy so that the design estimate for collector output on a typical winter day is 595 kWh thermal at 311° ±3°C.

The measured output of the collector on March 22, 1977, when peak radiation was 1 kW/m^2, was 431 kWh. Utilization of this 431 kWh in subsystems in a day is inventoried in Table I.

Tables I and II show that both electrical and thermal energy were produced from solar energy. The testing has also revealed areas to improve efficiency and reduce costs. Among these are

1. Improving collector efficiency
   a. Improvement of concentration optics
   b. Reduction of receiver heat losses
2. Reducing energy losses from the fluid loop and from thermal storage
3. Improving turbine/generator efficiency
4. Eliminating minor control problems
5. Reducing requirements for parasitic energy

Each of these is discussed in turn.

TABLE I

Winter Day Thermal Inventory, Phase IVA MSSTF

Direct Normal Solar Radiation	1550 kWh/Day
Measured Collected Thermal Energy	431 kWh/(March 22, 1977)
Efficiency Conversion of Solar to Thermal	27.8%

Use of Thermal Energy in Subsystems	kWh/Day	Percent of Total	Date of Test
Fluid Loop (loss)	57	13.2	April 4, 1977
Thermocline Storage[1] (loss)	72	16.7	January 10, 1977
Electrical Energy	35	8.1	Daily Average
Usable Thermal Energy	236	54.8	Daily Average
Residual Stored Thermal Energy[2]	31	7.2	Daily Average
	431	100.0	

[1] Unavailable energy in thermocline region - 28 kWh.
Energy lost through insulation - 44 kWh.

[2] Estimate

From Table I several efficiencies can be calculated:

TABLE II

Efficiency of Phase IVA MSSTF

Conversion	Formula	Efficiency (%)
Collected Thermal Energy to Electricity	$\frac{35}{431}$	8.1
Collected Thermal Energy to Usable Energy	$\frac{35 + 236}{431}$	62.9
Integrated Normal Solar Radiation to Electricity	$\frac{35}{1550}$	2.2
Integrated Normal Solar Radiation to Usable Energy	$\frac{35 + 236}{1550}$	17.4

Collector Operation, Problems, and Solutions

Marine plywood was selected for the support structure because it can be formed to required tolerances in existing facilities at less cost than other materials available.

The reflective surface chosen was aluminized Teflon bonded to Mylar and then to aluminum sheet. Although this surface has a lower reflectivity than glass, it is less expensive and much easier to form to the parabolic contour.

The receiver tube is an annulus formed by two mild-steel tubes. The outer tube must have sufficient diameter to intercept the sun's image on the focal line. The inner tube restricts the area through which fluid flows so as to cause the high fluid velocities necessary to create the turbulence required for good heat transfer. The outer tube is coated with the most effective selective coating known, black chrome. Surrounding the outer steel tube is a glass tube to reduce losses by convection. The annulus inside the glass tube can be evacuated for greater reduction in thermal energy losses.

The E-W parabolic trough collector field has been arranged and instrumented so the performance may be determined for each of four separate strings of 50 m^2 aperature (Figure 10a). The installed collector field has been exposed to the environment for more than 27 months and has been operated more than 2000 hours.

Experimental measurement of peak efficiencies has indicated ways to improve collector efficiency and life. The design goal for peak efficiency with 260 Pa (0.2 Torr) in the glass annulus surrounding the receiver is 60%; with atmospheric pressure, it is 55%.[3] Actual peak efficiencies are lower than this.

The equation for peak efficiency is:

$$\text{Peak Efficiency} = \frac{(\text{Flow Rate})\ (\text{Specific Heat})\ (\Delta T)^{*}}{(\text{Direct Normal Radiation})\ (\text{Area})} \tag{1}$$

All energy losses vary as a percentage of solar radiation with one exception. The loss from the receiver through the glass annulus is relatively constant as long as the temperature of the receiver remains constant.

The peak (solar noon) efficiencies for a 21-month period starting July 1976 for each string in the collector field subsystem (Figure 10a) are plotted on Figure 10b. The following observations were made.

1. Because the fluid flows sequentially through the northeast, southeast, southwest, and northwest strings, the downstream receivers experience higher operating temperatures. Discoloration of the receiver surfaces has been observed; it appears to worsen in the downstream direction.

---

*The cosine term is not included because peak efficiency occurs close enough to solar noon so that the effect of the cosine term is insignificant.

2. By July 13, 1976, the date of the first plotted test results, extensive replacement of receivers and reflector panels damaged by a windstorm in April 1976 had been accomplished. Except for the support structure, the collector field was virtually new.

3. The reflector surfaces were cleaned before all tests except the June 30, 1977 test.

4. Before June 30, new receivers were installed in the two west strings.

5. Before January 8, 1978, 20% of the reflector panels were replaced. After a visual inspection, the most degraded panels throughout the field were selected for replacement. During the test on January 8, 1978, the pressure in the annulus of the receivers on the two west strings was reduced to an average of 26 Pa (200 microns of mercury). A test conducted on the preceding day (January 7, 1978) with atmospheric pressure in the annulus resulted in lower efficiencies (about two percentage points) on the west strings, which shows that reducing pressure in the annulus increases efficiency.

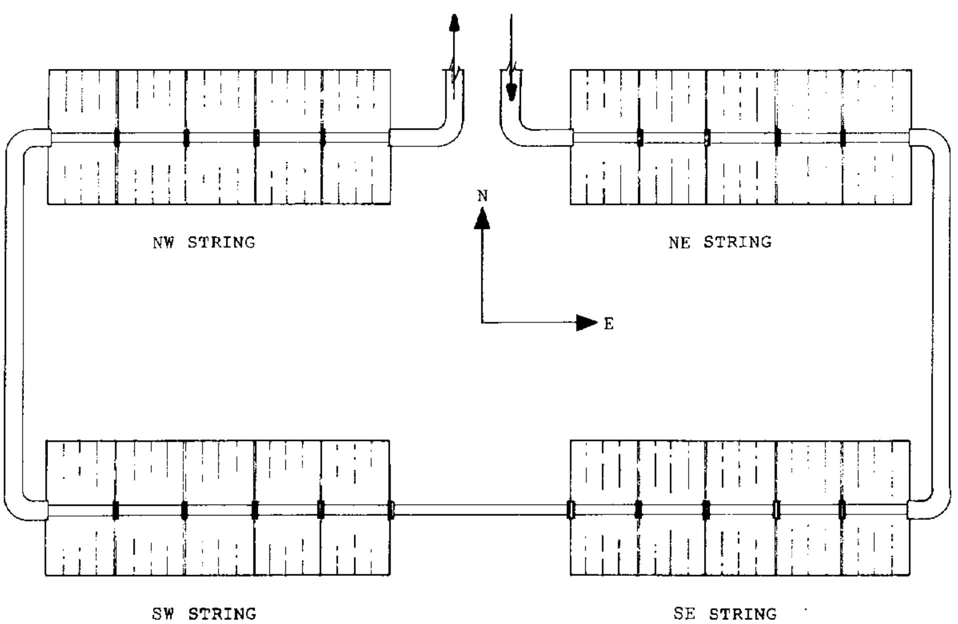

Figure 10a. E-W Parabolic Trough, Solar Collector Field

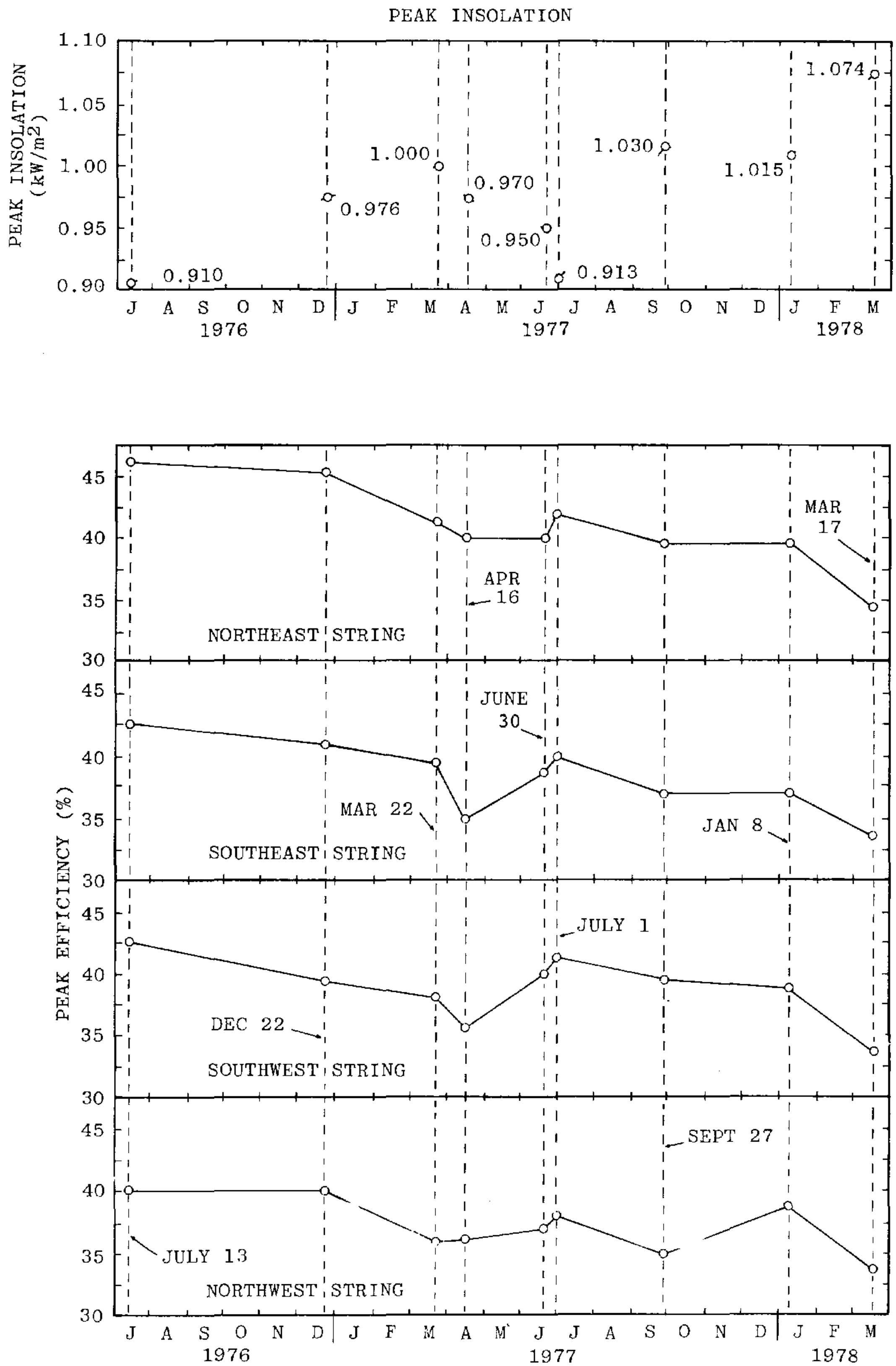

Figure 10b. Peak Efficiency by String of E-W Parabolic Trough, Collector Field Subsystem, July 1976 - March 1978

The following inferences can be drawn from the above observations:

1. MSSTF testing substantiates other experience, which indicates significant degradation of the standard, commercial black-chrome absorber surface as the operating temperature approaches 300°C, and the degradation rate is temperature-dependent.

2. On July 13, 1976, peak efficiency was below the design goal of 55%. As shown later, receiver thermal losses are relatively constant. Because of this, efficiency appears to decrease as solar radiation decreases. On July 13, 1976, the peak solar radiation was 913 W/m^2. If the observed efficiency on July 13 is normalized to 1000 W/m^2 it exceeds 50%.

3. Cleaning the reflectors between the June 30, 1977 and July 1, 1977 tests caused the most noticeable change in efficiency.

4. Between July 1976 and March 1978 many instances of replacement, repair, and modification occurred that should have improved performance. Instead, efficiences decreased, indicating an overall degradation within the collector field subsystem that offset improvement. Apparent degradation between January 8, 1978 and March 17, 1978 was particularly severe.

In addition to testing of the Phase IVA MSSTF as a system, there have been ancillary tests of components, collector materials, etc, in support of the project. Adding the results of such tests to the data from the system has helped to measure several aspects of the system operation:

- On the basis of laboratory measurements made on panels replaced in the collector field, the reflectivity of the second surface Teflon reflective coating (0.03-mm Teflon, vapor-deposited aluminum, and Mylar mounted on 0.6-mm aluminum sheet) decreased from a measured pretest value of 0.85 to an average measured value of 0.75.

- Not all the reflected energy strikes the receiver. No instruments exist to measure the amount of energy that misses the receiver. However, using data in this report, this quantity has been calculated to be 11.5%. Slit aperture tests[4] and tests during which the aperture was reduced by masking from 2.7 m (9 ft) to 2.1 m (7 ft) show that most of this loss results from distortion at the outer edges of the reflector. A slit aperture test covers the aperture except for a small slit. This slit admits light, the path of which can be followed visually. The slit can be moved to any position across the aperture. The masking test is one in which the outer edges of the receiver are masked to reduce the aperture from 2.7 m to 2.1 m, a reduction of 22%. A new efficiency is calculated using the reduced aperture area. Both tests verify that the quantity of reflected energy missing the receiver in the Phase IVA MSSTF configuration is approximately 11.5%.

- Transmissivity of the glass annulus surrounding the receiver tube has been reduced by dust and film from a measured 91% to an estimated 90%.

- Absorptivity of the black-chrome selective coating on the receiver tube has been reduced from a measured 95% to measured values that average 85% for all receivers. There was a reduction in emittance from 0.25 to about 0.18.[5]

- When the pressure in the annulus is increased from 26 Pa to atmospheric, (101.3 kPa), conduction losses are increased from a calculated 0.11 kW/m^2 (=0.29 kW/m of receiver) aperture to a measured 0.16 kW/m^2 (=0.43 kW/m of receiver). It is important to note that the thermal losses from the receiver are of particular concern because they are essentially functions only of the receiver surface temperature. Therefore, in all-day (or longer) operation of the collector, these losses do not diminish as the solar input is reduced from its peak value by atmospheric conditions or by geometric losses when the insolation is not normal to the collector aperture.

The measured efficiencies of the components of the collector as given above are plotted in Figure 11a with design estimates based on data from laboratory tests of the materials. In Figure 11b these efficiencies are converted into thermal loss rates when the insolation is 1 kW/m^2 and the temperature of the fluid leaving the receiver is 311°C.

One of the prime functions of a test facility is to discover in an experimental environment those system design features that fail to perform as expected. The test data as described above has identified some improvements that should be made before similar systems are considered for commercial applications. Often, the improvement involves simply substituting a more suitable component, and such system modifications are being made as time and hardware availability permit. Other improvements require the development of a process, material, apparatus, etc. The following developmental actions have been initiated as a result of testing experience.

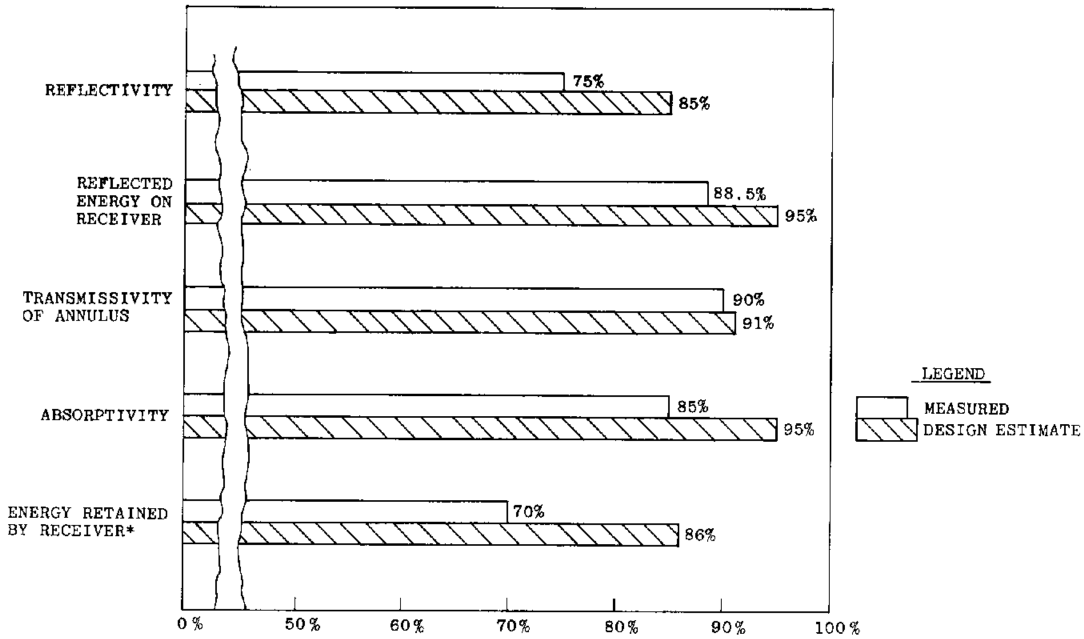

*THIS QUANTITY IS NOT A FUNCTION OF SOLAR RADIATION BUT IS A FUNCTION OF RECEIVER TEMPERATURE

Figure 11a. Design Estimates vs Measured Efficiencies, E-W Parabolic Trough Collector Subsystem (Peak Solar Radiation = 1000 W/m^2).

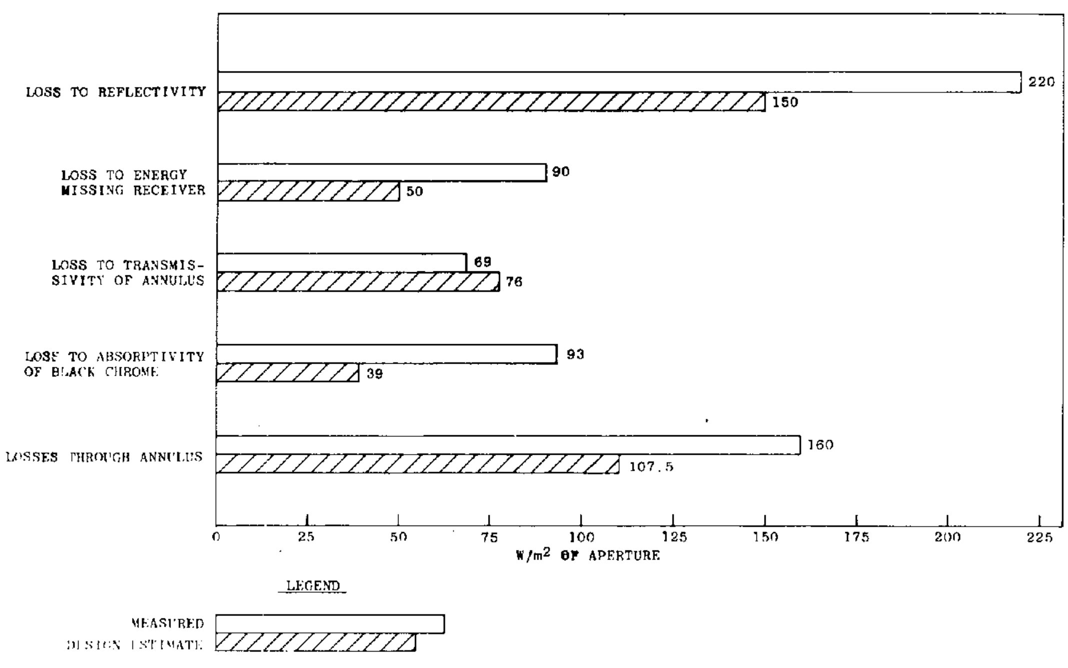

Figure 11b. Calculated Design and Measured Thermal Losses at Peak Efficiency, E-W Parabolic Trough Collector Subsystem (Peak Solar Radiation = 1000 W/m^2)

1. The second Teflon reflective surface will be replaced by glass with ~0.95 reflectivity. Thin glass is being developed in larger sizes that can be bent to shape rather than sagged as is now required.

2. Development is under way to replace one-half the E-W parabolic collector field support structure and reflector with an improved design and replace the other half of the field with collectors of a new design from the foundation up. Also, three different collector concepts have been or will be installed for evaluation in the Phase IVB MSSTF. These are the General Atomic (GA) Fixed Mirror Solar Collector (FMSC), the Suntec Solar Linear Array Thermal System (SLATS),[6] and two-axis tracking parabolic dishes by Raytheon and General Electric.

3. The observed degradation of the black-chrome absorber coating varies among receivers in a way not completely explained by the differences in operating temperatures experienced by the receivers. This points to a processing problem; i.e., a nonuniform coating rather than a basic materials problem. Intensive development is under way to define the problem and to find a solution.[5]

4. The MSSTF project is conducting studies to measure the effect of reduced pressure in the annulus around the receiver tube.[7]

Because of the research nature of MSSTF activities, there is an exaggerated emphasis (relative to a commercial system) on control, instrumentation, and data acquisition and handling. From operating the facility, several factors of this type have been identified as needing a higher degree of precision so that phenomena may be properly characterized and measured. While these factors are important to the interpretation of data, their effect on the system performance (i.e., the energy collected per day) is thought to be minor. Some of these observations are discussed below.

1. A delay occurs between a change in conditions (temperature of entering fluid, solar radiation, etc) and the time the result is sensed at the receiver exit. This limits the degree to which the output fluid temperature can be controlled at a constant value.

2. Only the position of the collector support is fed back to the tracking control system. Thus, there is no automatic mechanism to adjust the collector position if the receiver is not exactly on the focal line. Large errors are corrected manually, but small deviations may go unnoticed.

3. There has been no independent check on the manufacturer's published properties for T-66, either as received or after some use at operating temperatures.

4. Peak efficiency is directly related to flow rate (Equation 1, page 25). In the Phase IVA MSSTF there is no way to calibrate the flow meters under actual working conditions. However, there are two flow meters in series, and they are in good agreement.

5. Peak efficiency is a direct function also of difference in temperature (ΔT) between fluid entering the receiver and fluid leaving the receiver (Equation 1). Even small errors in measuring ΔT can have a significant impact on the determination of efficiency.

The following diagnostic and/or remedial actions are being taken as a result of the above observations.

1. We will develop a test plan to study the effect of variable output temperature from the receiver on total energy collected. There is already evidence that delivery of variable temperature fluid to a thermocline storage subsystem helps to start convection currents that degrade the thermocline.[8]

2. Efforts are under way to develop focusing equipment to measure the distribution of energy that strikes the receiver and causes the position of the collector to be adjusted automatically and to stay in focus.

3. Samples of the T-66 are being withdrawn from the system and sent to Mound Laboratory at Miamisburg, Ohio for characterization.

4. In the Phase IVB MSSTF, the multitank high-temperature storage subsystem will be equipped with instrumentation to measure continuous fluid level. Flow meters can be calibrated by pumping fluid into a thermal storage tank at a constant rate and measuring the change in volume in the thermal storage tank with respect to time.

5. Studies are under way in the CMTF to determine better ways to measure the temperature difference between entering and exiting fluid. Temperature measurements in the CMTF are more critical because ΔTs are smaller than in the MSSTF. Techniques learned there will be applied to the MSSTF.

Fluid-Loop Operation, Problems, and Solutions

Extensive evaluation of fabrication methods led to the use of welded Schedule 40 mild-steel tube rather than pipe to reduce thermal capacitance of the fluid-transfer system. Because of thermal expansion, it is necessary to provide support and anchors for the tubing. Conventional techniques (i.e., supports in contact with the tube and anchor welded to the tube) were selected because more energy-conservative techniques require retraining local craftsmen--an expensive, time-consuming, and unreliable process not warranted for such a small job.

Studies of various types of insulation led to the scheme depicted in Figure 12. Since the ceramic fiber insulation, Kaowool, could not be obtained preformed in time to meet schedules, the insulation had to be installed manually. A short training program was conducted for the craftsmen, but delays and pressures from other jobs caused the contractor to shift personnel, and not all the insulation was installed by trained craftsmen.

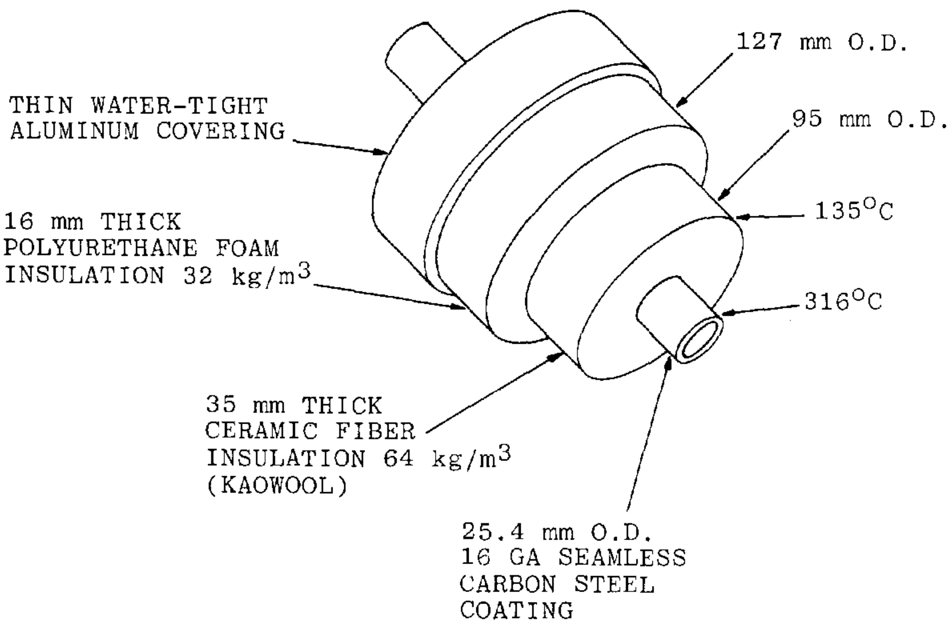

Figure 12. Construction of Insulated Pipeline, July 1976-January 1978

Losses from the fluid loop are approximately three times calculated design values. The reasons are:

1. Kaowool (Figure 12) was installed manually. Thus, density and thermal resistance are neither uniform nor within design values.

2. The metal support structures and anchors are in direct contact with the pipe, thus providing a low thermal resistance path to the ambient.

3. The uninsulated portions of valves were shown by infrared scans to lose energy.

4. Uninsulated and water-cooled pumps lose energy estimated at 6 kWh per pump per day.

The additional fluid-transfer equipment required for the Phase IVB MSSTF is shown partially complete as of January 10, 1978 (Figure 13). This equipment incorporates the following improvements:

1. Preformed fiberglass insulation is used for the pipes.

2. Support structures and anchors are insulated from the pipes.

3. Valves are better insulated.

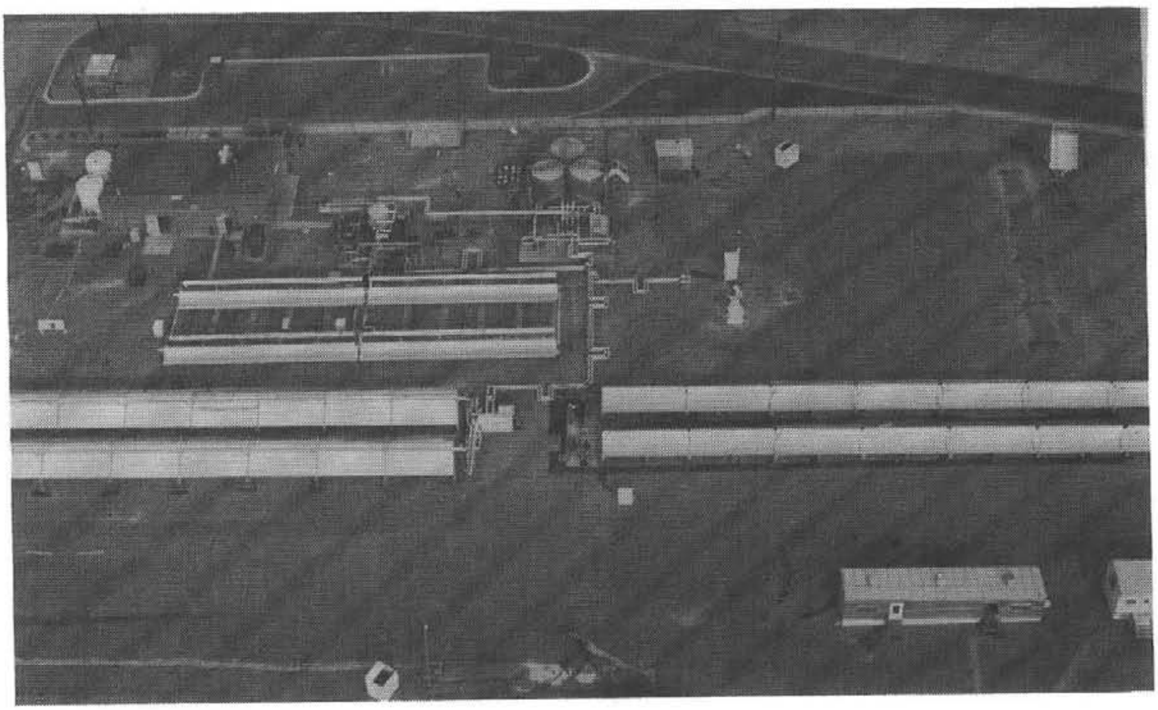

Figure 13. Aerial View of MSSTF, January 1978

Also, studies will be initiated to find ways to reduce energy losses from the pumps. With these improvements, the thermal loss from the fluid-transfer equipment of the Phase IVB MSSTF is estimated to be 4.3% of the collected energy, compared to 13.2% (Table I) measured for the Phase IVA MSSTF.

Thermal Storage Operation, Problems, and Solutions

The thermocline storage subsystem in the Phase IVA MSSTF was designed as a research tool to study storage of energy in high-pressure water or oil and to study the effectiveness of vacuum foil insulation.[8] Because of its capability to store water, the storage tank has thick walls that conduct energy vertically and contribute to thermocline degradation. The vacuum foil insulation has not reached its full effectiveness because leaks and/or outgassing of the foils preclude reducing the pressure in the annulus to the 1.3 Pa (10 microns of mercury) required to make the vacuum foil an effective insulator. Thermal loss from the thermocline storage subsystem was determined from measurements to be 16.7% of the collected energy.

The multitank high-temperature storage subsystem built for the Phase IVB MSSTF is designed to reduce thermal energy loss from storage to ≤6% of the total energy collected.

Prime-Mover Operation, Problems, and Solutions

As stated earlier, the prime mover comprises two elements: toluene heat exchanger and a turbine/generator.

The toluene heat exchanger, which consists of four compact heat exchangers, uses the hot T-66 to raise the temperature of the liquid toluene from condenser temperature to superheated vapor. The hot T-66 can be supplied from the collectors, from the thermal storage, or from the fossil-fired heater as shown in Figure 3.

Two pumps are required for the toluene heat exchanger: one to supply T-66 and one to supply the toluene. Both pumps consume parasitic power. Some reduction in pump power requirements can be achieved by using a larger heat exchanger. However, the disadvantage is slower response time.

The turbine/generator is a redesigned and modified 100-kW Sunstrand gas-fired toluene ORC machine. The fossil-fired toluene boiler was replaced by the toluene heat exchanger described above.

The test summary report[9] on the turbine/generator provides data on efficiency at different condenser inlet pressures and at different loads. In a total energy system, condenser inlet pressure is important because it affects the temperature at which thermal energy can be withdrawn from the condenser for use in other applications such as heating or operating an absorption chiller. A condenser pressure of 45 kPa (7 psia) provides condenser cooling fluid at a temperature of 68°C (155°F), which is adequate for winter space heating. A condenser pressure of 65 kPa (9 psia) supplies condenser cooling fluid at a temperature of 88°C (190°F), which will operate a lithium-bromide absorption chiller for summer space cooling.

Figure 14, taken from Reference 9, shows the effect on efficiency of varying condenser pressure and load. Note that changes in condenser pressure have a much smaller effect on turbine/generator efficiency than do changes in load.

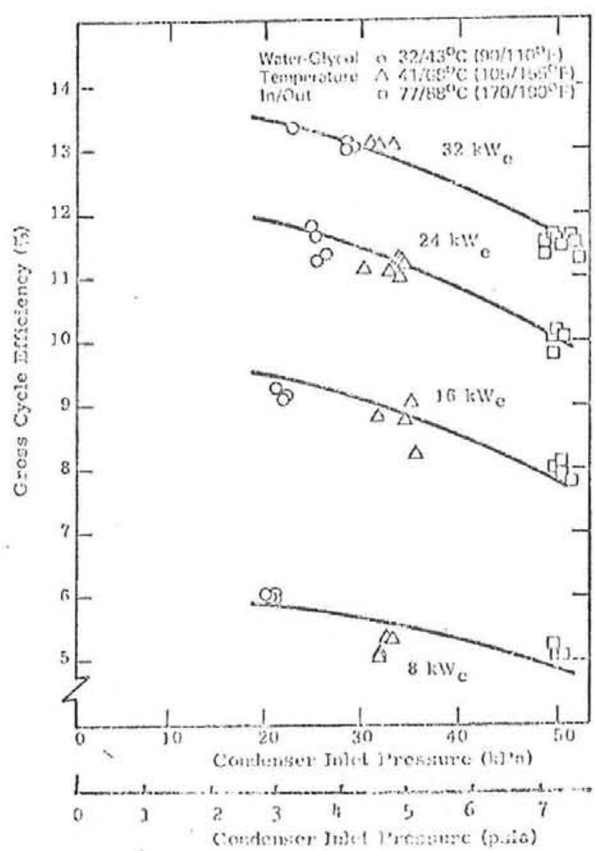

Figure 14. Turbine/Generator Gross Efficiency vs Condenser Pressure and Temperature

Reference 9 gives some of the major insights relating to the turbine/generator subsystem gained with an accumulation of more than 1800 operating hours.

<u>External Heat Exchanger</u> -- The use of an external, liquid-fired boiler is feasible. Because of the response lags inherent in a pumped-liquid heat source, there was concern that the turbine control system would have trouble accommodating sudden changes in load. Nevertheless, automatic control strategies have been devised that permit step increases from zero to full load and vice versa.

<u>Storage-to-Heater Switchover</u> -- Automatic control strategies have also been implemented that effect the switchover from storage to the gas-fired auxiliary heater as the high-temperature storage system becomes discharged, and the reverse as storage becomes fully charged from collector field output.

<u>Settable Condenser Temperature</u> -- Efficient operation of a solar total-energy system requires adjusting the temperature of the cascaded thermal energy to load requirements; otherwise an unnecessarily high condenser-coolant temperature would reduce the cycle efficiency of electrical power production. These techniques were also successfully demonstrated.

<u>Turbine Derating</u> -- The modification of an existing prime mover for reduced loads and operating temperature without substantial losses in efficiency has proved not feasible. For example, the turbine/generator installed at the MSSTF, designed for 100-kW output (maximum design electrical load at the MSSTFF is 32 kW), loses more than 10.4 kW in the gear box alone. A turbine tailored to a toluene superheated cycle at inlet temperature and pressure of about 310°C and 1.8 MPa (the conditions at the MSSTF) should be capable of cycle efficiencies of about 25%.[10] The existing turbine/generator operates at about half this value. The efficiency of the current turbine/generator will be increased for Phase IVB from 11.5% to 12.3% by reducing losses in the gear box.

Continuous Operation at Rated Power -- The most efficient operational setting is at rated power. Loads that require operation at rated power and minimize the need to accommodate sudden changes make possible the use of larger toluene heat exchangers and thereby reduce parasitic power requirements by reducing head loss through the toluene heat exchanger.

Parasitic Energy Concerns

In this report, parasitic energy losses are treated qualitatively rather than quantitatively, because the parasitic energy

- Operates items necessary for engineering evaluation but not for a facility that is strictly for the production of energy.

- Operates more equipment than is included in the Phase IVA MSSTF being discussed. For example, the air compressor supplies air to pneumatic controls in the larger Phase IVB MSSTF, which is being installed and checked out.

- Operates pumps that, because of the scaled-down size of the facility, are less efficient than pumps in a larger facility.

The item using the most parasitic energy is the motor to run the air compressor that supplies energy for remote operation of valves. This motor uses such large quantities of energy that it is a matter of major concern.

Some reasons for the high use of power by the air compressor can be traced to

- A variety of pneumatic controls installed at different times as the project progressed. Some are less efficient than others.

- Leaks in the air distribution system. Routine searches reveal leaks in threaded fittings that are immediately repaired.

- A high ratio of pneumatic-controlled valves to linear lengths of pipe. This high ratio is necessary to provide testing flexibility.

- Continuous air supply to pneumatic controls.

Recommended solutions to the above problems are:

1. Select from manufacturer's data the most efficient pneumatic controls and test them to assure that their use of air is within published specifications.

2. Avoid threaded joints in the air distribution system. Use soldered or brazed joints wherever possible.

3. Evaluate the trade-off between better control of the fluid-transfer equipment at the cost of more pneumatic controls vs poorer control as the result of using fewer pneumatic controls.

4. Valve off the air supply to pneumatic controls when they are not required (at night, for example).

Vacuum pumps are required for the insulation systems, such as the vacuum jacket around the high-temperature thermocline storage subsystem to maintain necessary low pressures. These vacuum pumps are the next largest user of parasitic power. Insulation systems that require the use of vacuum pumps should be avoided in solar energy applications. This does not preclude the use of vacuum in insulation since it is possible to establish a vacuum and maintain it in a properly sealed system without using vacuum pumps.

Much of the parasitic power is consumed by the numerous pumps in the system. Some pumps are included to provide experimental flexibility in the test facility. Excessive use of power for pumping, especially in prototype and commercial installations, may be remedied by minimizing the number of pumps, by using pumps of an appropriate size and design, and by reducing friction in flow passages (e.g., in heat exchangers and interconnecting piping).

Friction may be reduced by minimizing lengths of piping, by increasing cross-sectional areas, by using smooth surfaces, and by eliminating any unnecessary bends, valves, or junctions that might restrict flow. One of the more significant contributions of the MSSTF may be the fund of experience developing relative to the use of pumps in solar energy applications.

Predicted Performance of Phase IVB MSSTF

The Phase IVB MSSTF will contain the collector field systems listed in Table III, and, in parallel with the thermocline storage, a multitank high-temperature storage subsystem (Figure 19), which has a capacity of 860 kWh between 240° and 310°C.

TABLE III

Collectors in Phase IVB MSSTF

Collector Field Subsystem	Figure	Area (m^2)	Goal for Collector ($kWh/m^2/day$)	Capability[1] kWh/day
Eastern half of present parabolic troughs with new support structure and glass reflector surface	None[2]	100	3.0	300
Western half of present parabolic troughs new from foundation up	None[2]	100	3.3	330
General Atomic FMSC	15	260	2.3	600
Suntec SLATS	16	260	2.4	624
Raytheon Parabolic Dish	17	35	5.4	189
GE Parabolic Dish[3]	18	140	5.0	700
		895		2743

[1]Typical winter day

[2]Design is not complete

[3]Design is not yet frozen - prototype for large-scale experiment (LSE) at Shenandoah, GA (Reference 11)

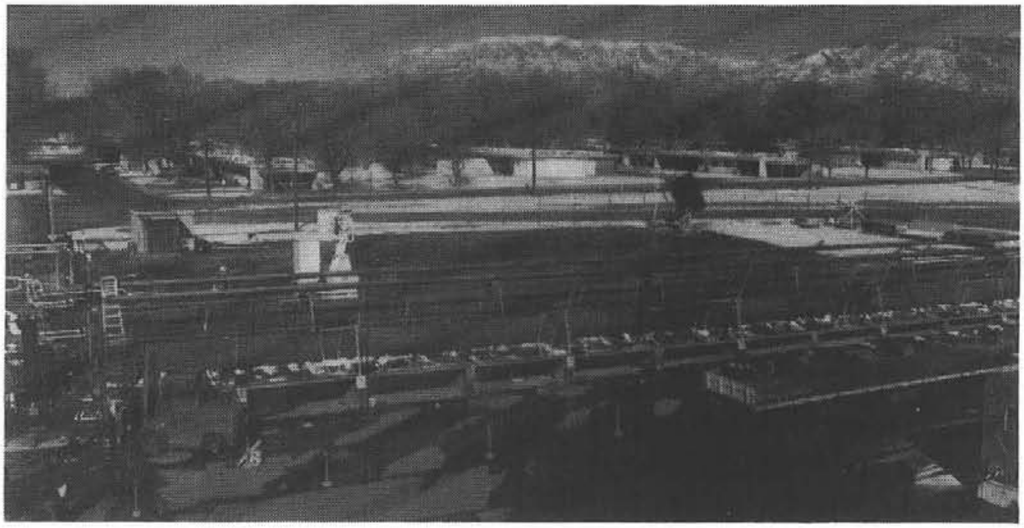

Figure 15. 260-m^2 General Atomic Fixed Mirror Solar Collector Field Subsystem, January 1978

Figure 16. 260-m^2 Sunctec SLATS Collector Field Subsystem, January 1978

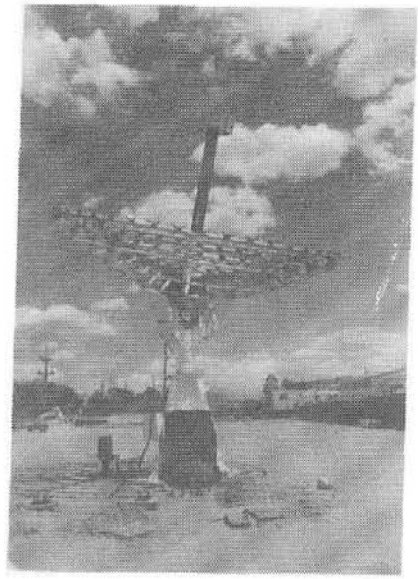

Figure 17. 35-m^2 Raytheon Parabolic Dish Collector (before installation of reflectors), April 1978

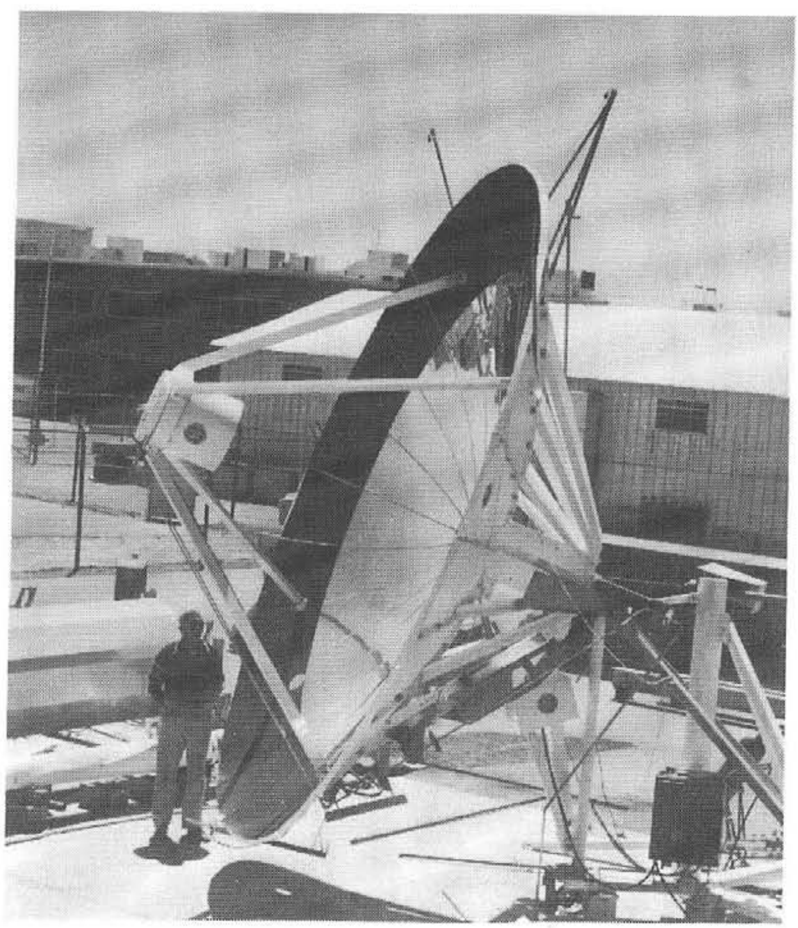

Figure 18. General Electric Parabolic Dish Collector in CMTF, April 1978

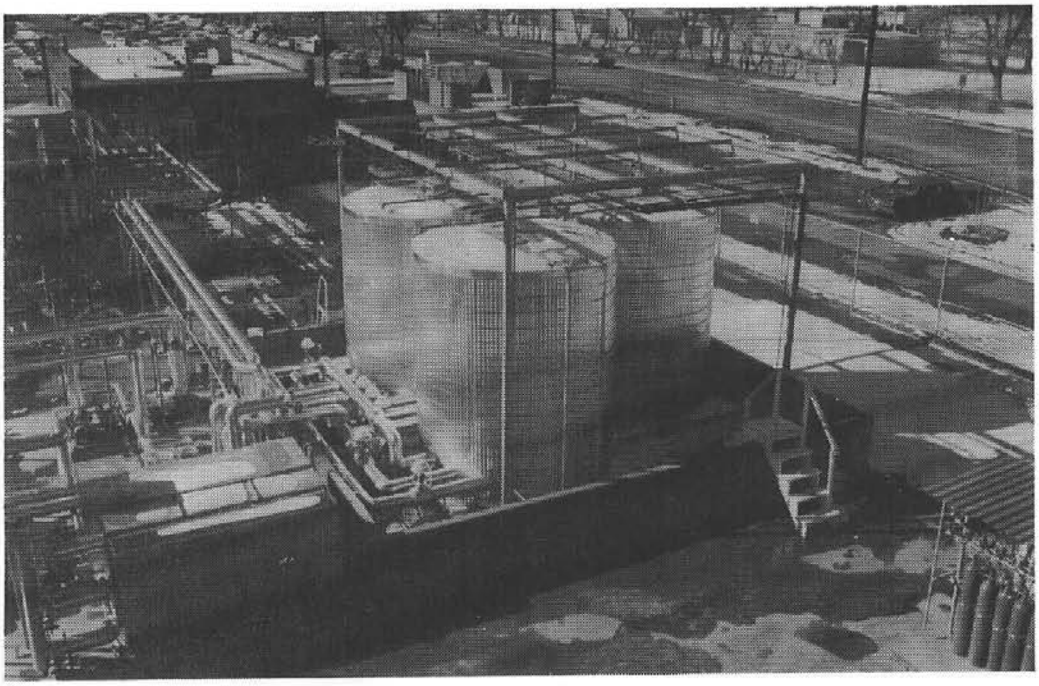

Figure 19. 860-kWh Multitank High-Temperature Thermal Storage Subsystem, January 1978

Based on the incorporation of the improvements previously described, the predicted winter-day collection capability for the Phase IVB MSSTF is given in Table IV, and an inventory of the energy used is given in Table V.

From Table III and the effect of applying techniques learned during Phase IVA, it is possible to predict in Table IV a thermal inventory for the Phase IVB MSSTF.

Table V compares the percent losses and energy produced in the Phase IVA MSSTF with those predicted for the Phase IVB MSSTF. Incorporation of techniques learned during Phase IVB should result in substantial improvement in producing usable energy in Phase IVB.

TABLE IV

Predicted Winter-Day Thermal Inventory, Phase IVB MSSTF

Direct Normal Solar Radiation	6936 kWh/day
Predicted Collection Capability	2743 kWh/day
Predicted Efficiency Solar to Thermal	39.5%

Predicted Use of Thermal Energy in Subsystem	kWh/day	Percent of Total
Fluid Loop Loss	114	4.3
Multitank Thermal Storage Loss	164	6.0
Electrical Energy (@ 12.3%)	288	10.6
Usable Thermal Energy	2047	74.7
Residual Stored Energy	120	4.4
	2743	100.0

TABLE V

Comparison, Winter-Day Thermal Inventory, Phase IVA MSSTF vs Phase IVB MSSTF

	Phase IVA MSSTF	Phase IVB MSSTF
Daily Efficiency, Solar to Thermal	27.8%	39.5%
Use in System	Percent of Collected Thermal Energy	
Loss in Fluid Loop	13.2	4.3
Loss in Thermal Storage	16.7	6.0
Electric Energy Produced	8.1	10.6
Usable Thermal Energy Produced	54.8	74.7
Residual Stored Energy	7.2	4.4
	100.0	100.0

Results and Conclusions

The MSSTF is designed to perform two prime experimental functions: To characterize components and subsystems that might be parts of dispersed solar power systems, and to integrate experimental hardware into representative systems for test and evaluation.

The fundamental conclusion to be drawn to date from the MSSTF testing relates to the integration function. It has been demonstrated that a system configured as in the Phase IVA MSSTF (Figure 2) can convert solar energy to electrical and thermal energy for a representative load. Also, feasible operational strategies have been developed for the system. Further, having demonstrated the feasibility of the overall concept of cascading solar energy through a system to provide both electrical and thermal energy, the design of the Phase IVA MSSTF is established as a baseline for developing system and component improvements. Demonstration of one viable system design does not preclude other approaches, but it does provide a standard by which new concepts may be judged.

With an acceptable system configuration, it is now possible to exercise the characterization function by assessing the performances of the many constituent parts in the context of an operating system. The results of the testing experience can be divided into two categories: (1) performance data on existing hardware, and (2) insights for improving subsequent hardware designs.

Performance data on specific components and subsystems are reported in detail in subsystem test reports (e.g., References 8 and 9). Systems test data obtained to date are summarized in this report.

Results of the "insight" type are particularly important at the present developmental status of dispersed solar power systems technology. Some of the more significant and fundamental insights are presented below. More detailed discussions of these and similar conclusions are available in other MSSTF reports.

1. Second Teflon reflective surfaces appear to be substantially inferior to glass in maintenance requirements and durability. Activities have been initiated to develop a highly reflective glass mirror, thin enough to be shaped to the concentrator contour.

2. The black chrome receiver surface coating produced for Phase IVA is not sufficiently stable at operating temperatures. In the past, black-chrome surfaces have been used primarily for decoration. An investigation has indicated that the conventional production process is not adequately controlled to assure a uniform product with respect to the characteristics desired for solar applications. A program is under way to develop the specification of a production process, and the fabrication of a facility, if necessary, that will yield a black-chrome coating more uniformly suitable to MSSTF receivers.

3. The thermocline high-temperature storage subsystem has demonstrated the feasibility of the thermocline concept; i.e., a thermocline can be established and maintained over a limited range of operational parameters. However, the tank was designed originally to contain either oil or water; to withstand the pressures associated with high-temperature water, the tank walls are 25 mm (1-in) thick. This permits enough vertical conduction of heat in the walls to compromise the thermocline severely over longer storage periods. Also, the multifoil vacuum insulation blanket around the tank has not proved satisfactory because of difficulties in reaching and maintaining a vacuum in the insulator.

4. Operation of the ORC turbine has demonstrated that it is feasible to operate the turbine with an elevated exhaust temperature, to vary the condenser conditions seasonally to match the requirements of the application, and to supply energy to the working fluid through a heat exchanger from a high-temperature liquid. It has also been shown that, to approach expected efficiences, the turbine must be designed for the application.

5. Because of the experimental nature of the project, somewhat increased thermal loss and consumption of parasitic power are expected. However, experience with the system indicates that these inefficiencies can be quite large and, even in commercial systems with minimum flexibility and diagnostic instrumentation, considerable design effort should be committed to minimizing parasitics and thermal losses.

6. The operation of the MSSTF has added considerable support to the plan of having a test facility in which to evaluate hardware before committing the design to larger projects. Although the tested hardware has undergone extensive studies and laboratory evaluation before installation at the MSSTF, the testing with few exceptions has revealed design flaws that would have had substantial negative cost or schedule impacts on the construction and operation of prototype or commercial installations.

References

1. J. A. Leonard, Operating Experience at the DOE/Sandia Midtemperature Solar Systems Test Facility, SAND78-0820C, 13th IECEC Symposium, San Diego, CA, August 1978.

2. K. D. McAllister and S. Thunborg, Solar Total Energy Test Facility Operational Phase Test Plan, SAND77-0696, Sandia Laboratories, Albuquerque, NM, May 1977.

3. R. W. Harrigan, Solar Total Energy Program Semiannual Report, October 1974-March 1975, SAND75-0278, Sandia Laboratories, Albuquerque, NM.

4. T. D. Harrison, (ed), Solar Total Energy System Facility Project, Semiannual Report, April 1976-September 1976, SAND76-0662, Sandia Laboratories, Albuquerque, NM, April 1977.

5. R. R. Sowell and R. B. Pettit, Thermal Aging of Electrodeposited Black Chrome, SAND78-0554, Sandia Laboratories, Albuquerque, NM, April 1978.

6. Suntec Systems, Inc., Sandia Total Energy Test Facility Project, Final Report, Sunctec 260 m^2 SLATS Subsystem, SAND78-7016, Suntec Systems Inc., 21405 Hamburg Avenue, Lakeville, MN, November 1977.

7. A. C. Ratzel, C. E. Hickox, and D. K. Gartling, "Techniques for Reducing Thermal Conduction and Natural Convection Heat Losses in Annular Receiver Geometrices," November 27-December 3, 1977, Winter Annual ASME Meeting, Altanta, GA.

8. T. D. Harrison, C. E. Hickox, A. Ortega, and K. Wally, Solar Total Energy Test Facility Project, Test Results, High Temperature Thermocline Thermal Storage Subsystem, SAND77-1528, Sandia Laboratories, Albuquerque, NM, April 1978.

9. J. P. Abbin, Solar Total Energy Test Facility Project, Test Results, Rankine Cycle Energy Conversion Subsystem, SAND78-0396, Sandia Laboratories, Albuquerque, NM, April 1978.

10. R. E. Barber, "Current Costs of Solar Powered Organic Rankine Cycle Engine," Solar Energy, Vol 20, No. 1, 1978, Pergamon Press, P. O. Box 52, Parkville, Victoria Australia 3052, pp. 1-5.

DISTRIBUTION:
TID-4500-R66, UC62 (316)

Aerospace Corporation
101 Continental Blvd.
El Segundo, CA 90245
Attn: E. L. Katz

Acurex Aerotherm
485 Clyde Avenue
Mountain View, CA 94042
Attn: G. J. Neuner

Solar Total Energy Program
American Technological University
P. O. Box 1416
Killeen, TX 76541
Attn: B. L. Hale

Argonne National Laboratory (3)
9700 South Cass Avenue
Argonne, IL 60439
Attn: R. G. Matlock
W. W. Schertz
R. Winston

Atlantic Richfield Co.
515 South Flower Street
Los Angeles, CA 90071
Attn: H. R. Blieden

Barber Nichols Engineering
6325 W. 55th Avenue
Arvada, CO 80002
Attn: R. G. Olander

Battelle Memorial Institute
Pacific Northwest Laboratory
P. O. Box 999
Richland, WA 99352
Attn: K. Drumheller

Brookhaven National Laboratory
Associated Universities, Inc.
Upton, LI, NY 11973
Attn: J. Blewett

Congressional Research Service
Library of Congress
Washington, DC 20540
Attn: H. Bullis

Del Manufacturing Co.
905 Monterey Pass Road
Monterey Park, CA 91754
Attn: M. M. Delgado

Desert Research Institute
Energy Systems Laboratory
1500 Buchanan Blvd.
Boulder City, NV 89005
Attn: J. O. Bradley

Desert Sunshine Exposure Inc.
P. O. Box 185
Phoenix, AZ 85020
Attn: G. A. Zerlaut

Honorable P. V. Domenici
Room 405
Russell Senate Office Bldg.
Washington, DC 20510

Edison Electric Institute
90 Park Avenue
New York, NY 10016
Attn: L. O. Elsaesser
Director of Research

Energy Institute
1700 Las Lomas
Albuquerque, NM 87131
Attn: T. T. Shishman

EPRI
3412 Hillview Avenue
Palo Alto, CA 94303
Attn: J. E. Bigger

General Atomic
P. O. Box 81608
San Diego, CA 92138
Attn: J. L. Russell

General Electric Company
Valley Forge Space Center
Valley Forge, PA 19087
Attn: W. Pijawka

General Electric Co.
P. O. Box 8661
Philadelphia, PA 19101
Attn: A. J. Poche

Georgia Institute of Technology
School of Mechanical Engineering
Atlanta, GA 30332
Attn: S. P. Kezios, President
American Society of
Mechanical Engineers

DISTRIBUTION: (cont)

Georgia Institute of Technology
Atlanta, GA 30332
Attn: J. D. Walton

Georgia Power Company
Atlanta, GA 30302
Attn: W. Hensley
Vice President Economics Services

Grumman Corporation
4175 Veterans Memorial Highway
Ronkonkoma, NY 11779
Attn: E. Diamond

Hexcel
11711 Dublin Blvd.
Dublin, CA 94566
Attn: G. P. Branch

Jet Propulsion Laboratory
4800 Oak Grove Drive
Pasadena, CA 91103
Attn: V. C. Truscello

Kingston Industries Corporation
205 Lexington Avenue
New York, NY 10016
Attn: K. Brandt

Lawrence Berkeley Laboratory
University of California
Berkeley, CA 94720
Attn: M. Wallig

Los Alamos Scientific Laboratory (3)
P. O. Box 1663
Los Alamos, NM 87545
Attn: J. D. Balcomb
C. D. Bankston
D. P. Grimmer

Honorable M. Lujan
1324 Longworth Building
Washington, DC 20515

Mann-Russell Electronics, Inc.
1401 Thorne Road
Tacoma, WA 98421
Attn: G. F. Russell

Martin-Marietta Aerospace
P. O. Box 179
Denver, CO 80201
Attn: R. C. Rozycki

McDonnell Douglas Astronautics Co.
5301 Bolsa Avenue
Huntington Beach, CA 92647
Attn: D. Steinmeyer

NASA-Lewis Research Center
Cleveland, OH 44135
Attn: R. Hyland

New Mexico State University
Las Cruces, NM 88001
Attn: R. L. San Martin

Oak Ridge Associated Universities
P. O. Box 117
Oak Ridge, TN 37830
Attn: A. Roy

Oak Ridge National Laboratory (4)
P. O. Box Y
Oak Ridge, TN 37830
Attn: J. R. Blevins
C. V. Chester
J. Johnson
S. I. Kaplan

Office of Technology Assessment
Old Immigration Building, Rm 722
119 D. Street, NE
Washington, DC 20002
Attn: H. Kelly

Omnium G (2)
1815 Orangethorpe Park
Anaheim, CA 92801
Attn: R. Derby
S. P. Lazzara

PRC Energy Analysis Company
7600 Old Springhouse Road
McLean, VA 22101
Attn: W. N. Luddy

Rocket Research Company
York Center
Redmond, WA 98052
Attn: R. J. Stryer

DISTRIBUTION: (cont)

Honorable H. Runnels
1535 Longworth Building
Washington, DC 20515

Honorable H. H. Schmitt
Room 1251
Dirksen Senate Office Bldg.
Washington, DC 20510

Scientific Atlanta, Inc.
3845 Pleasantdale Road
Atlanta, GA 30340
Attn: A. L. Blackshaw

Sensor Technology, Inc.
21012 Lassen Street
Chatsworth, CA 91311
Attn: I. Rubin

Solar Energy Research Institute (7)
1536 Cole Blvd.
Golden, CO 80401
Attn: C. J. Bishop
K. Brown
B. L. Butler
F. Kreith
C. Grosskreutz
B. P. Gupta
A. Rabl

Solar Energy Technology
Rocketdyne Division
6633 Canoga Avenue
Canoga Park, CA 91304
Attn: J. M. Friefeld

Solar Kinetics Inc.
P. O. Box 10764
Dallas, TX 75207
Attn: G. Hutchison

Southwest Research Institute
P. O. Box 28510
San Antonio, TX 78284
Attn: D. M. Deffenbaugh

Stanford Research Institute
Menlo Park, CA 94025
Attn: A. J. Slemmons

Stone & Webster
Box 5406
Denver, CO 80217
Attn: V. O. Staub

Sun Gas Company
Suite 800, 2 No. Pk. E
Dallas, TX 75231
Attn: R. C. Clark

Sundstrand Electric Power
4747 Harrison Avenue
Rockford, IL 61101
Attn: A. W. Adam

Sunsearch, Inc.
669 Boston Post Road
Guilford, CT 06437
Attn: E. M. Barber, Jr.

Suntec Systems Inc.
21405 Hamburg Avenue
Lakeville, MN 55044
Attn: J. H. Davison

Swedlow, Inc.
12122 Western Avenue
Garden Grove, CA 92645
Attn: E. Nixon

TEAM Inc.
8136 Ola Keene Mill Road
Springfield, VA 22152

US Department of Energy (2)
Agricultural & Industrial Process Heat
Conservation & Solar Application
Washington, DC 20545
Attn: W. W. Auer
J. Dollard

US Department of Energy (3)
Albuquerque Operations Office
P. O. Box 5400
Albuquerque, NM 87185
Attn: D. K. Nowlin
G. Pappas
J. R. Roder

US Department of Energy
Division of Energy Storage Systems
Washington, DC 20545
Attn: C. J. Swet

DISTRIBUTION: (cont)

US Department of Energy (9)
Division of Solar Technology
Washington, DC 20545
Attn: R. H. Annan
G. W. Braun
H. Coleman
M. U. Gutstein
G. M. Kaplan
L. Melamed
J. E. Rannels
M. E. Resner
J. Weisiger

US Department of Energy
Los Angeles Operations Office
350 S. Figueroa Street, Suite 285
Los Angeles, CA 90071
Attn: F. A. Glaski

US Department of Energy
San Francisco Operations Office
1333 Broadway, Wells Fargo Bldg.
Oakland, CA 94612
Attn: J. Blasy

University of California
Lawrence Livermore Laboratory
P. O. Box 808
Livermore, CA 94500
Attn: W. C. Dickinson

University of Delaware
Institute of Energy Conversion
Newark, DE 19711
Attn: K. W. Boer

University of New Mexico (2)
Department of Mechanical Eng.
Albuquerque, NM 87113
Attn: W. A. Cross
M. W. Wilden

Watt Engineering Ltd.
RR1, Box 183 1/2
Cedaredge, CO 81413
Attn: A. D. Watt

Western Control Systems
13640 Silver Lake Drive
Poway, CA 92064
Attn: L. P. Cappiello

Westinghouse Electric Corp.
P. O. Box 10864
Pittsburgh, PA 15236
Attn: J. Buggy

1100	C. D. Broyles
1472	L. G. Rainhart
1500	W. A. Gardner
1520	T. L. Pace
1530	W. E. Caldes
1540	R. L. Brin
1550	F. W. Neilson
1552	O. N. Burchett
2300	J. C. King
2320	K. L. Gillespie
2323	C. M. Gabriel
2324	L. W. Schulz
2326	G. M. Heck
3161	J. E. Mitchell
3600	R. W. Hunnicutt
	Attn: H. H. Pastorius, 3640
3700	J. C. Strassel
4000	A. Narath
4200	G. Yonas
4231	J. H. Renken
4700	J. H. Scott
4710	G. E. Brandvold
4713	B. W. Marshall
4714	R. P. Stromberg
4715	R. H. Braasch
4719	D. G. Schueler
4720	V. L. Dugan
4721	J. A. Leonard (300)
4722	J. F. Banas
4723	W. P. Schimmel
4730	H. M. Stoller
5512	H. C. Hardee
5520	T. B. Lane
5524	R. T. Othmer
5600	D. B. Shuster
5630	R. C. Maydew
5800	R. S. Claassen
	Attn: R. G. Kepler, 5810
	R. E. Whan, 5820
5830	M. J. Davis
5831	N. J. Magnani
5834	D. M. Mattox
5840	H. J. Saxton
5842	J. N. Sweet
5844	F. P. Gerstle, Jr.
5846	E. K. Beauchamp

DISTRIBUTION: (Cont)

8400	L. Gutierrez
8450	R. C. Wayne
8451	W. G. Wilson
8452	A. C. Skinrood
8266	E. A. Aas
3141	T. L. Werner (5)
3151	W. L. Garner (3)
	For DOE/TIC (Unlimited Release)